Submitted to Journal "BUILDING AND ENVIRONMENT"

INFLUENCE OF AIR SUPPLY PARAMETERS ON INDOOR AIR DIFFUSION

QINGYAN CHEN*
PETER SUTER*
ALFRED MOSER*

This paper presents the field distributions of air velocity, temperature, contaminant concentration, and thermal comfort in an office with displacement ventilation for different air supply parameters such as the effective area, shape, and dimension of the diffuser and the turbulence intensity, flow rate, and temperature of the air supplied. The research is conducted numerically by using an airflow computer program based on a low-Reynolds-number k-ε model of turbulence. It can be concluded that the effective area, shape, and dimension of the diffuser and the turbulence intensity of the air supplied have little effect on the room air diffusion except at the floor level. The influence of the flow rate and temperature of the air supplied is very significant on the air diffusion as well as on the thermal comfort and indoor air quality.

NOMENCLATURE

A_{C1}, A_t, A_μ	turbulence model constants
C_1, C_2, C_3, C_μ	turbulence model constants
f_1, f_2, f_μ	turbulence model functions
g_i	gravity in i direction
H	enthalpy
I	turbulence intensity
k	kinetic energy of turbulence
m	mass inflow rate
PD	percentage dissatisfied people due to draft
R_k	turbulence Reynolds number ($k^{1/2}y/\nu_l$)
R_t	turbulence Reynolds number ($k^2/\nu_l\varepsilon$)
S_k, S_ε	source terms in k and ε equations due to buoyancy
T	air temperature
T_o	reference temperature
t	general time
V	mean velocity
V_i, V_j	mean velocity components in i and j direction
x_i, x_j	tensor notation for space coordinates
y	the smallest distance from a cell centre to a wall
β	expansion coefficient
ε	dissipation rate of turbulence energy
ν_l	laminar kinetic viscosity
ν_t	turbulent kinetic viscosity

* Energy Systems Laboratory, Swiss Federal Institute of Technology, ETH-Zentrum, CH-8092 Zurich, Switzerland.

ρ	density
$\sigma_H, \sigma_k, \sigma_\varepsilon$	turbulent Prandtl numbers for energy, turbulence energy, and dissipation rate of turbulence energy

1. INTRODUCTION

ENERGY CONSERVATION measures, resulting in tighter building envelopes and use of the materials with better thermal insulation, increase the concentrations of internally-generated contaminants in offices. Displacement ventilation systems have been therefore introduced to remove the contaminants more effectively. In the displacement ventilation systems, the air is supplied into a room in such a way that it fills the occupied zone with clean air. This can be done if it is supplied with low velocity (mostly less than 0.5 m/s) and with an air temperature at least 1°C lower than that in the occupied zone. As the supply air is colder than the air in the occupied zone, it will fill the lower part of the room because of gravity. The displacement ventilation systems have two advantages compared with traditional well-mixed systems, i.e. a more efficient use of energy [1] and a more appropriate routing of contaminated air [2]. A general description of the displacement ventilation systems has been given by skaaret [3].

With displacement ventilation, the supply air diffuser is of low-momentum. The diffuser can be a flat, rectangular unit, a quarter- or semicircle-cylindrical shape unit, or something else. Even for the same shape diffusers, the supply velocity profile and turbulence intensity can be very different [4]. In addition, the dimension and effective area of the diffuser, ventilation rate, and supply air temperature may have an impact on the indoor air diffusion. Since the air diffusion is related to comfort in a room, it is necessary to study the air diffusion under different air supply parameters. The main aim of the present paper is to study the influence of the variation of air supply parameters on air diffusion, indoor air quality, and thermal comfort. This is a part of the work carried out in the International Energy Agency Annex 20 - "Air flow pattern within buildings".

2. RESEARCH APPROACH

Studies of the air diffusion in a room for various kinds of air supply parameters are obtained by two main approaches: experimental investigation and numerical calculation. The most realistic information concerning diffuser characteristics and indoor airflow is, in principle, given by direct measurement. Some experimental research in this field has been conducted by Nielsen *et al.* [4]. An experimental investigation of the indoor air diffusion for different air supply parameters often requires a full-scale climate room in order to reveal air velocity, temperature, turbulence intensity, and pollutant concentration distributions. Such full-scale tests are, in most cases, expensive and some of the measurements present serious difficulties in many situations. These include the measurement of the flow direction at low velocity and the turbulence intensity. Moreover, the measuring instruments are not free from errors. Previous researchers have also noted that it is impossible to develop an undistorted similitude model for room air motion when there is internal heat production within the room, because the Reynolds number (ratio of inertial force to viscous force) and Archimedes number (ratio of thermal buoyancy force to viscous force) - both important dimensionless terms in determining room air distribution - lead to contradictory scaling factors.

Due to the limitations of the experimental approach and to the development of digital computer systems, numerical calculations of airflow and heat transfer in a

room have been used extensively in recent years. Encouraging results have been achieved by using numerical solutions for a number of problems concerning the airflow in a room as reviewed by Whittle [5] and Nielsen [6]. With the numerical techniques, it is possible to study the influence of air supply parameters on the field distributions of air velocity, temperature, turbulence intensity, and contaminant concentration in a room, and consequently, on the thermal comfort and indoor air quality.

In the numerical techniques, approximations are often required in the conservation equations of motion in order to make them solvable. For example, the details of turbulent flow are difficult to calculate and engineers are mainly interested in the mean values. Therefore, one turns to so-called turbulence models by which it is possible to compute the mean values. Recent results [7, 8] indicate that one of the turbulence models, the k-ε model of turbulence developed by Launder and Spalding [9], is still the most appropriate model for practical flow applications. The set of model equations is suitable for high-Reynolds-number flow. For the airflow in a room with displacement ventilation, where overall Reynolds numbers are very low and boundary layers are neither fully turbulent and well-developed nor completely laminar, disagreements have been found between measurements and predictions [10]. Therefore, it is necessary to apply an appropriate low-Reynolds-number model of turbulence for the computations of the air diffusion in a room with a displacement ventilation system.

In addition to the low-Reynolds-number property, buoyancy is also one of the dominant factors for the airflow in a room with displacement ventilation systems. Besides the buoyancy term in the momentum equation, the buoyancy production terms in the equations of turbulence energy and turbulence dissipation rate also interact with the transportation of momentum and energy. Hence, it is also necessary to introduce buoyancy production terms in the equations of the kinetic energy of turbulence (k) and the dissipation rate of turbulence energy (ε).

In the present study, the airflow program developed by Rosten and Spalding [11] has been employed to calculate air distribution. The computations involve the solution of three-dimensional equations for the conservation of mass, momentum (u, v, w), energy (H), contaminant concentration (C), turbulence energy (k), and the dissipation rate of turbulence energy (ε). The turbulence model used is a low-Reynolds-number k-ε model [12] with buoyancy production terms in the k and ε equations [13] as detailed in [14]. The model has been implemented in the airflow program and verified to be more suitable for indoor airflow simulations, and a better agreement between computation and experiment has been found with respect to velocity and turbulence energy distributions and heat exchange through solid walls [14]. In the model, the transport equations of the kinetic energy (k) and the dissipation rate of turbulence energy (ε) are:

$$\frac{Dk}{Dt} = \frac{\partial}{\partial x_j}\left[\left(\frac{\nu_t}{\sigma_k} + \nu_l\right)\frac{\partial k}{\partial x_j}\right] + \nu_t\left(\frac{\partial V_i}{\partial x_j} + \frac{\partial V_j}{\partial x_i}\right)\frac{\partial V_i}{\partial x_j} - \varepsilon + S_k \tag{1}$$

$$\frac{D\varepsilon}{Dt} = \frac{\partial}{\partial x_j}\left[\left(\frac{\nu_t}{\sigma_\varepsilon} + \nu_l\right)\frac{\partial \varepsilon}{\partial x_j}\right] + C_1 f_1 \nu_t \frac{\varepsilon}{k}\left(\frac{\partial V_i}{\partial x_j} + \frac{\partial V_j}{\partial x_i}\right)\frac{\partial V_i}{\partial x_j} - C_2 f_2 \frac{\varepsilon^2}{k} + S_\varepsilon \tag{2}$$

$$S_k = \beta \frac{\nu_t}{\sigma_H}\frac{\partial (T - T_o)}{\partial x_i} g_i \tag{3}$$

$$S_\varepsilon = C_3 \frac{\varepsilon}{k} S_k \tag{4}$$

The time-averaged flow field can be determined through the eddy viscosity given by:

$$\nu_t = C_\mu f_\mu k^2/\varepsilon \tag{5}$$

where $\sigma_H = 0.9$, $\sigma_k = 1.0$, $\sigma_\varepsilon = 1.3$, $C_1 = 1.44$, $C_2 = 1.92$, $C_3 = 1.44$, and $C_\mu = 0.09$.

In fact, these equations are a general form of those given by Launder and Spalding [9] in which the functions f_μ, f_1, and f_2 are all assumed to be identically one. This assumption cannot be valid within a laminar sub-layer or in low-Reynolds-number flows. The functions f_μ, f_1, and f_2 are given by the following equations:

$$f_\mu = (1 - e^{-A_\mu R_k})^2 \left[1 + \frac{A_t}{R_t} \right] \tag{6}$$

$$f_1 = 1 + \left[\frac{A_{C1}}{f_\mu} \right]^3 \tag{7}$$

$$f_2 = 1 - e^{-R_t^2} \tag{8}$$

where the turbulence model constants are $A_\mu = 0.0165$, $A_t = 20.5$, and $A_{C1} = 0.05$, and R_k and R_t are turbulence Reynolds numbers.

When a low-Reynolds-number k-ε model is applied, no wall function formulae are required because the model is valid for the whole flow domain. However, the boundary conditions for k and ε must be specified. We have tested a number of methods as reviewed by Patel *et al.* [15] but it is very difficult to obtain converged and correct results. In the present study, the wall function formulae are used, but the distance between the wall and the first grid can be very small. This indicates that the first grid points will be located inside the viscous layer. In the viscous sublayer, the wall function formulae express linear velocity and temperature distributions and which can be accepted for airflow in a room. In this circumstance, the second and even the third grid points may still be in the inner region of the boundary layer and the low-Reynolds-number model will work well for those points. This is different from the application of the high-Reynolds-number model in combination with the wall function formulae in which the first grid must be sufficiently remote from the wall.

Fanger *et al.* [16] pointed out that the turbulence of an airflow has a significant impact on the sensation of draft, and a mathematical model of draft risk including turbulence intensity was developed. The model predicts the percentage of people dissatisfied due to draft as a function of mean air velocity, turbulence intensity, and air temperature. In the model, the percentage dissatisfied people due to draft, *PD*, is calculated from:

$$PD = (34 - T)(V - 0.05)^{0.62} (3.14 + 0.37\, V I) \quad (\%) \tag{9}$$

for $V < 0.05$ m/s insert $V = 0.05$ m/s, for $PD > 100\%$ use $PD = 100\%$, where T is the local air temperature (°C), V is the mean velocity (m/s), and I is the turbulence intensity (%). The turbulence intensity is defined as the velocity fluctuation over the

mean velocity. The relationship between the turbulence intensity, I, and turbulence energy, k, can be written as:

$$I = 100\ (2k)^{0.5}/\ V \qquad (\%) \tag{10}$$

The T, V and k can be obtained from the airflow computation, and therefore, the PD distribution due to draft can be determined.

With the above mentioned method, we have studied the air diffusion for variations of the following air supply parameters: the effective area, shape, and dimension of a diffuser and the turbulence intensity, flow rate, and temperature of the air supplied.

3. RESULTS

The numerical computations have been carried out for two different size offices (one is 5.6 m long, 3.0 m wide, and 3.2 m high and the other is 4.5 m in length, 4.5 m in width and 2.5 m in height). For each office at least three computations have been done for changing each parameter of air supply. However, only the results from the second office, as shown in Figure 1, are presented in this paper since the conclusions from the results of the two offices are the same. The second office is with some furniture, two computers, and two occupants. For simplicity, no aerodynamic blockage is used for the computers. The contaminant from the occupant a is represented by a nominal contaminant source of 0.01 ml/s. To simulate a smoking person the computed concentration caused by the occupant may be scaled according to the ratio of the actual to the nominal source strength of a particular contaminant. The inside surface temperatures of the enclosures are 22.3°C. To simulate a summer cooling situation, a convective heat gain of 150 W is assumed from the window inner surface due to solar radiation. The heat source from each occupant is 80 W and from each computer 120 W.

Figure 2 shows the results for the office with the displacement ventilation system. The inlet size is 0.6 m in width and 0.6 m in height. The inlet, a flat, non-spreading diffuser, is assumed to be a simple grille with the effective area equal to the gross area. The turbulence intensity of the air supplied is 40%. The supply airflow rate is 70 l/s or 5 ach with a supply temperature of 19.0°C.

There are three large circulations as shown in sub-figure 2a. It is different from the assumption that there is only one eddy in an office with a displacement ventilation system. The heat sources from the computer and human body induce a large stream of air and smoke up to the ceiling. There is a marked temperature stratification in the office as illustrated in sub-figures 2c and 2d. Olesen *et al.* [17] pointed out that a 3°C of temperature difference between head (1.1 m) and ankles (0.1 m) will lead to a 6% of dissatisfaction. Thus the thermal comfort is still acceptable under this situation. Since the air stream generated by the heat sources forms a large eddy, it brings contaminated air downwards along the side wall. The complex flow pattern mixes the air well and a higher contaminant concentration is found in the upper part of the occupied zone of the office as illustrated in sub-figure 2e. However, the air quality in the lower part of the room is very good. If the room is with a high ceiling, the unpolluted air could occupy in a level higher than 1.80 m. Hence, the displacement ventilation system looks much more suitable for a room with a high ceiling. From sub-figure 2f, we can see that the smoke concentration is low in the left part of the office although there is a smoker on the right side of the tables. This is because the room geometry and heat sources are symmetrical and the room air is not well mixed. Melikov [20] pointed out that, in rooms with displacement ventilation, highest mean velocities were measured near the floor: 0.033 and 0.1 m. Therefore, it is necessary to study the air diffusion within this area.

Sub-figures 2g and 2h show the distributions of velocity and percentage dissatisfied people due to draft at the level 0.05 m above the floor. In this case, the percentage dissatisfied people due to draft near the inlet is still less than 15%. This is because the air velocity in the inlet is low (0.2 m/s) and the supply temperature is rather high (19.0°C). Those conditions are certainly in favour of comfort.

In the following sub-sections, the above mentioned case will be taken as a standard case. The influence of the air supply parameters such as the effective area, shape, and dimension of the diffuser and the turbulence intensity, flow rate and temperature of the air supplied on air diffusion will be studied. A summary of the cases is given in Table 1.

3.1. *Effective area*

Since the effective area of a diffuser is generally much smaller than the gross area, the actual air momentum through the supply opening is higher than that through a simple grille. The higher momentum entrains the room air near the supply opening and a longer projection is expected. In the airflow program, the inlet momentum, mV_{in}, is set as:

$$m\,V_{in} = m \text{ (volume inflow rate) / (effective area)} \qquad (11)$$

Equation (11) is a mathematical model for simulating a diffuser. In this numerical approach, every cell face of the inlet is, in fact, characterized by a fraction expressing the ratio of the effective area over gross area of the diffuser. The fraction determines what portion of each cell face is available for occupancy by the air, and what portion of each cell-face area can permit flow normal to it, by convection or diffusion, from one cell to its neighbour. A spreading diffuser can be simulated by setting air supply direction for each cell of the inlet. By giving different kinds of supply momentum and initial directions, different diffusers can be simulated. However, this method may not applied to a diffuser with very complex geometry.

Figure 3 is the results for the office but with a supply of smaller effective area than the standard case as shown in Figure 2. In this case, the ratio of the effective area to the gross area is 0.5. Since the air supply momentum is twice as high, the air velocity near the inlet is higher. However, the velocity decay is very fast and the values of the air momentum are absolutely low. The influence of the effective area of the inlet is limited to a small region only near the inlet. As shown in Figure 3, in the most part of the office, the field distributions of air velocity, temperature, contaminant concentration, and percentage dissatisfied people due to draft is the same as those shown in Figure 2.

3.2. *Shape*

The diffuser for displacement ventilation can be a flat, rectangular unit, a quarter- or semicircle-cylindrical shape unit, or something else. Different diffusers impose different boundary conditions in numerical simulations. This is carried out by presenting different momentum values and directions of air supply for each flow cell of the inlet. In this sub-section, a spreading diffuser is simulated. The supply angle varies from 0 to ±60° from the diffuser central section to its edges.

The field distributions of air velocity, temperature, contaminant concentration, and percentage dissatisfied people due to draft for this case are illustrated in Figure 4. Compared with Figure 2, it is obvious that the spreading diffuser spreads the flow over the whole width of the room and no re-circulation is found in the corners of the rear wall. With the wide spreading, the primary air mixes well with the room air and the velocity decay is faster. Nielsen *et al.* [4] found that the velocity decay can be given as a function of the Archimedes number. Because the air velocities at the level 0.05 m above the floor are smaller at a given distance, thermal comfort is better. Nevertheless, the difference is not very evident. Sub-figures 2a to 2f and 4a

to 4f indicate that the shape of the diffusers have little influence on the air diffusion in the upper part of the room.

3.3. *Turbulence intensity*

Fanger *et al.* [16] have shown that the thermal comfort is influenced by mean air velocity and by turbulence intensity. We have computed three cases with values of the supply turbulence intensity of 0%, 40%, and 100%. The results are the same except in the region a few centimetres from the inlet. Although the turbulence intensity of 100% is very high, the corresponding turbulence energy is very low because of the low velocity of air supplied. The contribution of the turbulence intensity from the diffusers to the space air diffusion is therefore neglectful under these circumstances.

From Equation (9) we can see that the value of V/I is important to thermal comfort. If the mean air velocity is low, the thermal comfort is still satisfied even with a high turbulence intensity. In the present study, the mean air velocity of the diffuser is 0.2 m/s. The largest difference of the dissatisfied people due to draft is less than 3% if the turbulence intensity varies from 0% to 100%.

3.4. *Diffuser dimension*

In order to study the influence of the diffuser dimension on space air diffusion, four computational results are shown in Figures 5 to 8. Figure 5 is with a smaller inlet height (0.3 m) and Figure 6 with a larger height (1.0 m). The width of the inlet for Figure 7 is 0.3 m and for Figure 8 is 1.0 m. The dimension of the diffuser for the standard case (Figure 1) is 0.6 m in width and height.

The smaller the diffuser dimension, the higher the velocity of air supply. The higher momentum entrains the room air near the supply diffuser and the overall air velocities at the floor level are larger as shown in sub-figures 5g and 7g. As a consequence, the percentage dissatisfied people due to draft is higher (sub-figures 5h and 7h. On the other hand, a large amount of room air is entrained such that the eddies in the corners of the rear wall become bigger. As the dimension of the diffuser is getting larger, the two eddies are vanishing. Comparing Figures 5 and 7 or Figures 6 and 8, we can see that the velocity distributions at the floor level are very similar because the diffuser area is the same. This implies that the diffuser geometry is not very important for air diffusion if the area is the same. From Figures 2, 5 to 8, we can conclude that the inlet dimension have little influence on the air diffusion except at the floor level. However, this conclusion may only apply for the airflow in a space with displacement ventilation. Since when the dimension becomes much smaller, the airflow from the inlet is of the jet flow type. Chen *et al.* [18] and others reported that the inlet momentum of a jet flow is one of the dominant factors influencing indoor air diffusion.

3.5. *Ventilation rate and supply temperature*

In this office, the heat gain is constant. If ventilation rate is higher, the supply air temperature must be higher too in order to maintain the same room air temperature at the centre of the occupied zone. In the standard case, the ventilation rate is 5.0 ach and the supply temperature is 19.0°C. Two additional cases, one with a 3.5 ach of ventilation rate and 17.0°C supply temperature and the other with 8.0 ach and 21.0°C, are setup here in order to study the influence of ventilation rate and supply temperature on air diffusion.

The computational results for the two additional cases are shown in Figures 9 and 10. Although the ventilation rates and supply temperatures vary a lot, the airflow patterns are very similar as shown in sub-figures a and b in Figures 9, 2, and 10. Ventilation rate is not the only factor influencing air diffusion. Supply flow momentum is much more important. In the present study, low flow momentum is

maintained for displacement ventilation. Therefore, the airflow patterns are similar for different ventilation rates.

From sub-figures c and d in Figures 9, 2, and 10, we can see that, the smaller the ventilation rate or the lower the supply air temperature, the larger the vertical air temperature gradient. However, the temperature gradient is not inversely proportional to the ventilation rate. The case with 3.5 ach ventilation rate is not acceptable from the view point of thermal comfort because of the large vertical temperature gradient.

The computed results presented in sub-figures e and f in Figures 9, 2, and 10 show that the larger the ventilation rate, the better the indoor air quality. This is obvious. There is a large vertical gradient of concentration in the mid height of the room. It is very difficult to decrease the gradient or to move it to the upper part of the room by increasing the ventilation rate. There are only two contours in sub-figure 10e but the gradient is still large. This is because the overall concentration of the room is low with a 8.0 ach of ventilation rate. For example, the concentration in the air extracted is 0.09 ppm for the case with a 8.0 ach of ventilation rate, 0.14 ppm with a 5.0 ach of ventilation rate, and 0.20 ppm with a 3.5 ach of ventilation rate. The product of the concentration difference between the upper and lower zone and the ventilation rate seems to be constant in the three cases. The experimental results reported by Chen *et al.* [19] do not show a large concentration gradient in the mid height of the room. In their study, helium is used as tracer gas and the helium concentration is relatively high (about 5000 ppm in the air extracted). Since the helium density is much lower than air density, the buoyancy force caused by the density difference between the helium and room air has an effect on concentration distribution. Therefore, it should be avoided to use a large amount of tracer gas that has different density from air to simulate a contaminant.

When the ventilation rate is lower, the flow spreads wider at the floor level because the air supply momentum is smaller. As a result, the eddies in the two corners of the rear wall are smaller (sub-figures g in Figures 9, 2, and 10). Since the mean velocities are lower at the floor level, the values of percentage dissatisfied people due to draft are reduced as shown in sub-figures h in Figures 9, 2, and 10.

4. CONCLUSIONS

Several cases of numerical simulation were conducted to examine the influence of different air supply parameters such as the effective area, shape, and dimension of a diffuser and the turbulence intensity, flow rate, and temperature of the air supplied on the air diffusion in an office with displacement ventilation. The main results of the study are summarized as follows.

- The effective area, shape, and dimension of the diffuser and the turbulence intensity of the air supplied have little contribution to room air diffusion except at the floor level. The airflow in the room can be divided into two zones, the upper zone and lower zone. The upper zone seems to be irrelevant to those air supply parameters. The lower zone is directly effected by these parameters and can be studied separately.
- The influence of the flow rate and temperature of the air supplied is very significant on the air diffusion as well as on the thermal comfort and indoor air quality. For a given space heat gain, the ventilation rate and the temperature of the air supplied are coupled parameters. Too low ventilation rates with corresponding low supply temperatures result in a high vertical temperature gradient and therefore are not recommended for practical applications due to the requirement of thermal comfort. The room air diffusion, thermal comfort, and indoor air quality are very sensitive to the ventilation rate and supply temperature.

Acknowledgement -- This investigation was financially supported by the Swiss Federal Office of Energy (BEW).

REFERENCES

1. Q. Chen, T. G. Hoornstra, and J. van der Kooi, Energy analysis of buildings with different air supply and exhaust systems. *ASHRAE Transactions*, **96** (1) (1990).
2. M. Sandberg and C. Blomqvist, Displacement ventilation systems in office rooms, *ASHRAE Transactions*, **95** (2) (1989).
3. E. Skaaret, Displacement ventilation. Proceedings of ROOMVENT-87 International Conference on Air Distribution in Ventilated Spaces, Stockholm (1987).
4. P. V. Nielsen, L. Hoff, L. G. Pedersen, Displacement ventilation by different types of diffusers. Proceedings of the 9th AIVC Conference on Effective Ventilation, Vol. 2, Gent (1988).
5. G. E. Whittle, Computation of air movement and convective heat transfer within buildings. *International Journal of Ambient Energy*, **3**, 151-164 (1986).
6. P. V. Nielsen, Progress and trends in air infiltration and ventilation research. Proceedings of the 10th AIVC Conference on Progress and Trends in Air Infiltration and Ventilation Research, pp. 165-184, Dipoli (1989).
7. Special Issue, Numerical solutions of fluid problems related to buildings, structures and the environment. *Building and Environment*, **24**, 3-110 (1989).
8. N. Rhodes, Prediction of smoke movement: an overview of field models. *ASHRAE Transactions*, **95** (1) (1989).
9. B. E. Launder, and D. B. Spalding, 1974. The numerical computation of turbulent flows. *Computer methods in applied mechanics and engineering*, **3**, 269-289 (1974).
10. Q. Chen, *Indoor Airflow, Air Quality and Energy Consumption of Buildings.* Ph.D. Thesis, Delft University of Technology, Delft, 1988.
11. H. I. Rosten and D. B. Spalding, The PHOENICS Reference Manual, CHAM TR/200, CHAM Ltd, London (1987).
12. C. K. G. Lam and K. Bremhorst, A modified form of the k-ε model for predicting wall turbulence. *Journal of Fluids Engineering*, ASME Transactions. **103**, 456-460 (1981).
13. P. V. Nielsen, A. Restivo, and J. H. Whitelaw, Buoyancy-affected flows in ventilated rooms. *Numerical Heat Transfer*, **2**, 115-127 (1979).
14. Q. Chen, A. Moser and A. Huber, Prediction of natural convection in a room by a low-Reynolds-number k-ε model. *ASHRAE Transactions*, **96** (1) (1990).
15. V. C. Patel, W. Rodi, and G. Scheuerer, G. Turbulence models for near-wall and low Reynolds number flows: A review. *AIAA Journal*, **23**, 1308-1319 (1985).
16. P. O. Fanger, A. K. Melikov, H. Hanzawa and J. Ring, Turbulence and draft. *ASHRAE Journal*, **31** (7), 18-23 (1989).
17. B. W. Olesen, M. Scholer, and P. O. Fanger, Discomfort caused by vertical air temperature difference. Proceedings of Indoor Climate, Danish Building Research Institute, pp. 531-539, Copenhagen (1979).
18. Q. Chen, A. Moser, and P. Suter, Indoor air quality and thermal comfort under six kinds of air diffusion, submitted to *ASHRAE Transactions*, 1990.
19. Q. Chen, J. van der Kooi, and A. Meyers, Measurements and computations of ventilation efficiency and temperature efficiency in a ventilated room. *Energy and Buildings*, **12** (2), 85-99, (1988).

20. A. K. Melikov, G. Langkilde, and B. Derbiszewski, Airflow characteristics in the occupied zone of rooms with displacement ventilation. *ASHRAE Transactions*, **96** (1) (1990).

Table 1. Description of the air supply parameters of the cases studied

Case Section	$\dot{m}_{in}$ ach	Area ratio* -	Angle -	Height m	Length m	I %	Results Figure
3	5.0	1.0	0°	0.6	0.6	40	2
3.1	5.0	0.5	0°	0.6	0.6	40	3
3.2	5.0	1.0	0 - ±60°	0.6	0.6	40	4
3.3	5.0	1.0	0°	0.6	0.6	0, 100	-
3.4	5.0	1.0	0°	0.3	0.6	40	5
3.4	5.0	1.0	0°	1.0	0.6	40	6
3.4	5.0	1.0	0°	0.6	0.3	40	7
3.4	5.0	1.0	0°	0.6	1.0	40	8
3.5	3.5	1.0	0°	0.6	0.6	40	9
3.5	8.0	1.0	0º	0.6	0.6	40	10

* Area ratio is defined as the effective area over the gross area of the diffuser.

FIGURE CAPTIONS

Figure 1. Sketch of the office.

Figure 2. Computed field distributions in the office. (a) velocity in section I-I; (b) velocity in section III-III; (c) temperature in section I-I [°C]; (d) temperature in section III-III [°C]; (e) smoke concentration in section II-II [ppm]; (f) smoke concentration in section III-III [ppm]; (g) velocity in 0.05 m above the floor (top view); (h) percentage dissatisfied people due to draft in 0.05 m above the floor (top view) [%].

Figure 3. Computed field distributions with a smaller effective area. (a) velocity in section I-I; (b) velocity in section III-III; (c) temperature in section I-I [°C]; (d) temperature in section III-III [°C]; (e) smoke concentration in section II-II [ppm]; (f) smoke concentration in section III-III [ppm]; (g) velocity in 0.05 m above the floor (top view); (h) percentage dissatisfied people due to draft in 0.05 m above the floor (top view) [%].

Figure 4. Computed field distributions with different air supply angles. (a) velocity in section I-I; (b) velocity in section III-III; (c) temperature in section I-I [°C]; (d) temperature in section III-III [°C]; (e) smoke concentration in section II-II [ppm]; (f) smoke concentration in section III-III [ppm]; (g) velocity in 0.05 m above the floor (top view); (h) percentage dissatisfied people due to draft in 0.05 m above the floor (top view) [%].

Figure 5. Computed field distributions with a smaller inlet height. (a) velocity in section I-I; (b) velocity in section III-III; (c) temperature in section I-I [°C]; (d) temperature in section III-III [°C]; (e) smoke concentration in section II-II [ppm]; (f) smoke concentration in section III-III [ppm]; (g) velocity in 0.05 m above the floor (top view); (h) percentage dissatisfied people due to draft in 0.05 m above the floor (top view) [%].

Figure 6. Computed field distributions with a larger inlet height. (a) velocity in section I-I; (b) velocity in section III-III; (c) temperature in section I-I [°C]; (d)

temperature in section III-III [°C]; (e) smoke concentration in section II-II [ppm]; (f) smoke concentration in section III-III [ppm]; (g) velocity in 0.05 m above the floor (top view); (h) percentage dissatisfied people due to draft in 0.05 m above the floor (top view) [%].

Figure 7. Computed field distributions with a smaller inlet width. (a) velocity in section I-I; (b) velocity in section III-III; (c) temperature in section I-I [°C]; (d) temperature in section III-III [°C]; (e) smoke concentration in section II-II [ppm]; (f) smoke concentration in section III-III [ppm]; (g) velocity in 0.05 m above the floor (top view); (h) percentage dissatisfied people due to draft in 0.05 m above the floor (top view) [%].

Figure 8. Computed field distributions with a larger inlet width. (a) velocity in section I-I; (b) velocity in section III-III; (c) temperature in section I-I [°C]; (d) temperature in section III-III [°C]; (e) smoke concentration in section II-II [ppm]; (f) smoke concentration in section III-III [ppm]; (g) velocity in 0.05 m above the floor (top view); (h) percentage dissatisfied people due to draft in 0.05 m above the floor (top view) [%].

Figure 9. Computed field distributions with a smaller ventilation rate and a lower supply temperature. (a) velocity in section I-I; (b) velocity in section III-III; (c) temperature in section I-I [°C]; (d) temperature in section III-III [°C]; (e) smoke concentration in section II-II [ppm]; (f) smoke concentration in section III-III [ppm]; (g) velocity in 0.05 m above the floor (top view); (h) percentage dissatisfied people due to draft in 0.05 m above the floor (top view) [%].

Figure 10. Computed field distributions with a larger ventilation rate and a higher supply temperature. (a) velocity in section I-I; (b) velocity in section III-III; (c) temperature in section I-I [°C]; (d) temperature in section III-III [°C]; (e) smoke concentration in section II-II [ppm]; (f) smoke concentration in section III-III [ppm]; (g) velocity in 0.05 m above the floor (top view); (h) percentage dissatisfied people due to draft in 0.05 m above the floor (top view) [%].

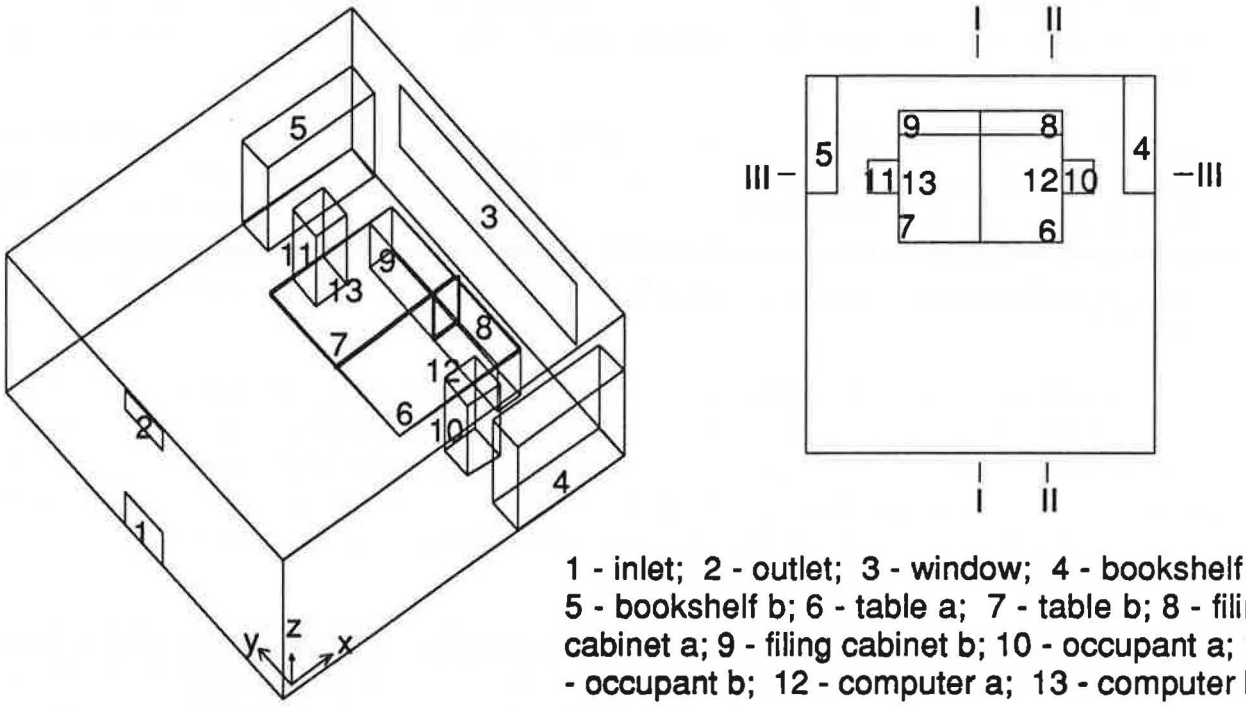

1 - inlet; 2 - outlet; 3 - window; 4 - bookshelf a; 5 - bookshelf b; 6 - table a; 7 - table b; 8 - filing cabinet a; 9 - filing cabinet b; 10 - occupant a; 11 - occupant b; 12 - computer a; 13 - computer b.

Figure 1. Sketch of the office

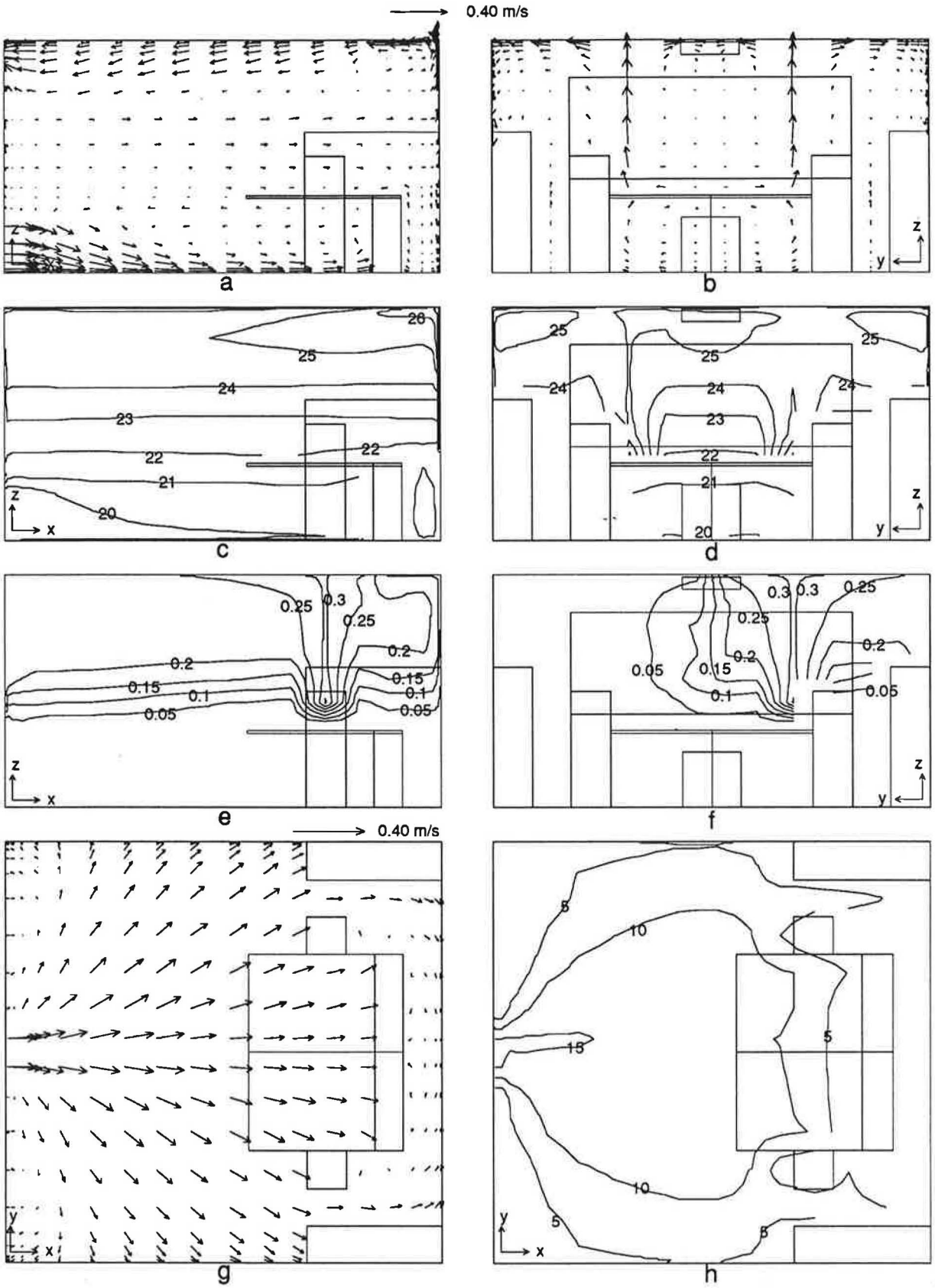

Figure 2. Computed field distributions in the office. (a) velocity in section I-I; (b) velocity in section III-III; (c) temperature in section I-I [°C]; (d) temperature in section III-III [°C]; (e) smoke concentration in section II-II [ppm]; (f) smoke concentration in section III-III [ppm]; (g) velocity in 0.05 m above the floor (top view); (h) percentage dissatisfied people due to draft in 0.05 m above the floor (top view) [%].

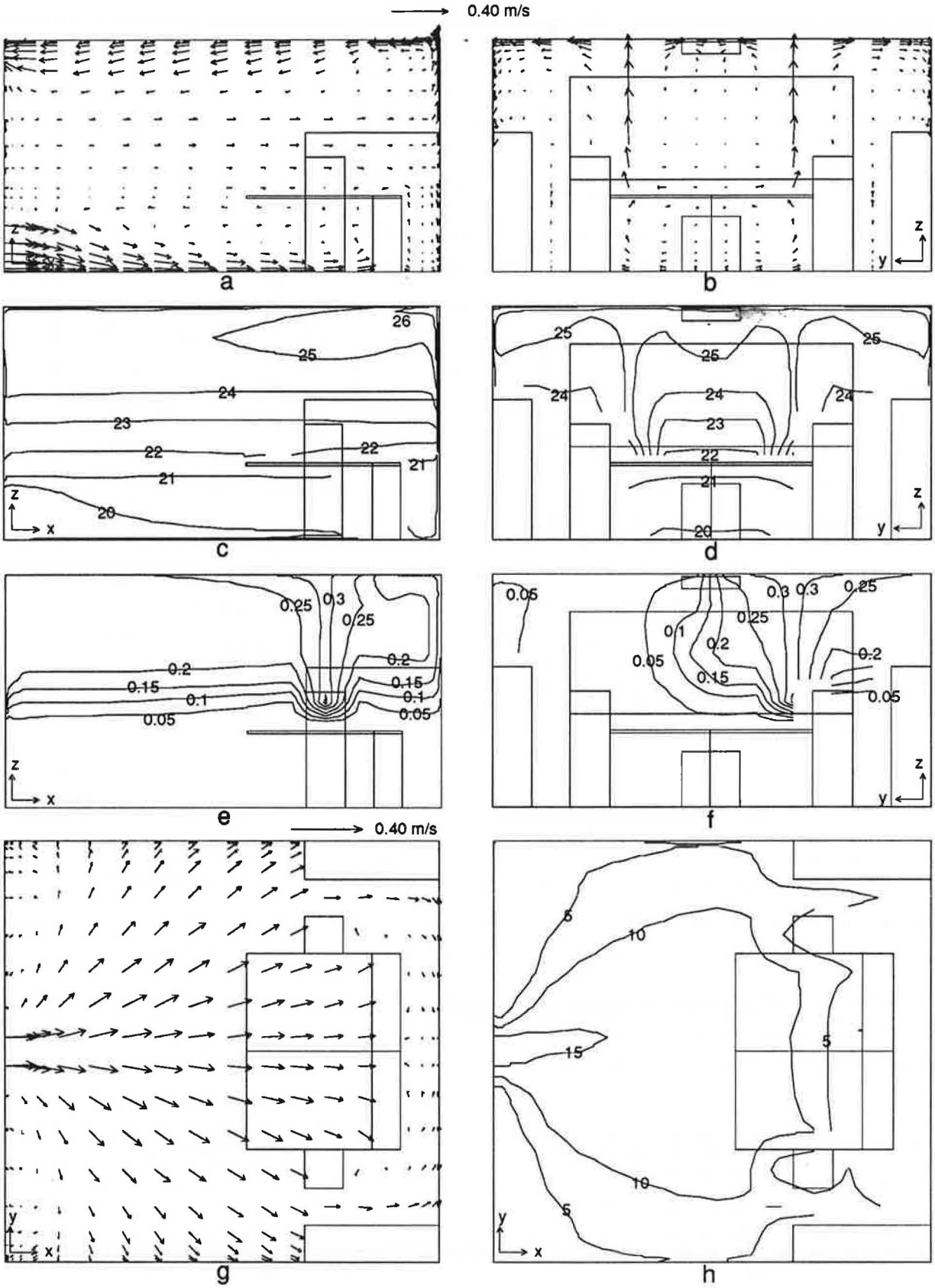

Figure 3. Computed field distributions with a smaller effective area. (a) velocity in section I-I; (b) velocity in section III-III; (c) temperature in section I-I [℃]; (d) temperature in section III-III [℃]; (e) smoke concentration in section II-II [ppm]; (f) smoke concentration in section III-III [ppm]; (g) velocity in 0.05 m above the floor (top view); (h) percentage dissatisfied people due to draft in 0.05 m above the floor (top view) [%].

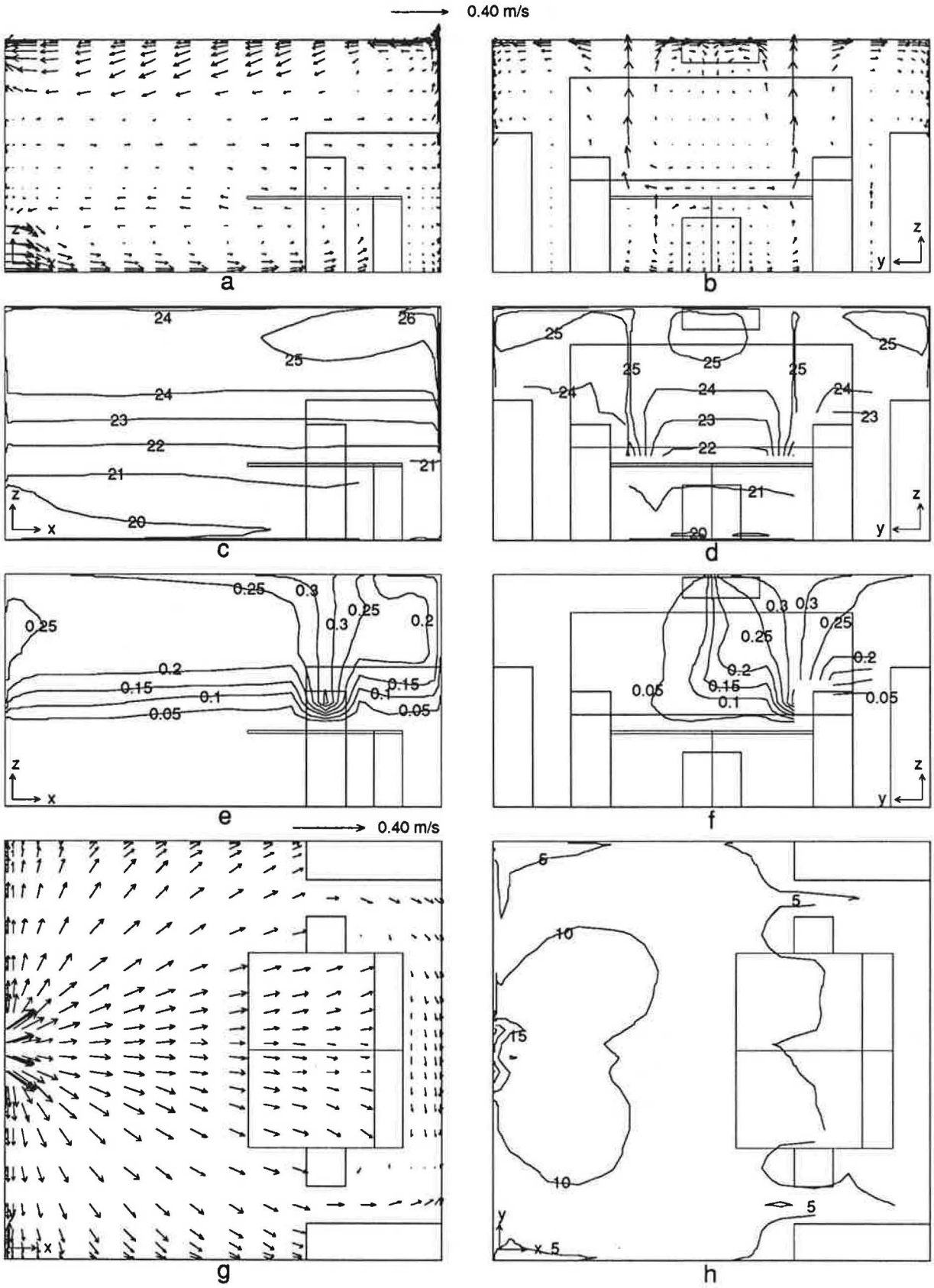

Figure 4. Computed field distributions with different air supply angles. (a) velocity in section I-I; (b) velocity in section III-III; (c) temperature in section I-I [℃]; (d) temperature in section III-III [℃]; (e) smoke concentration in section II-II [ppm]; (f) smoke concentration in section III-III [ppm]; (g) velocity in 0.05 m above the floor (top view); (h) percentage dissatisfied people due to draft in 0.05 m above the floor (top view) [%].

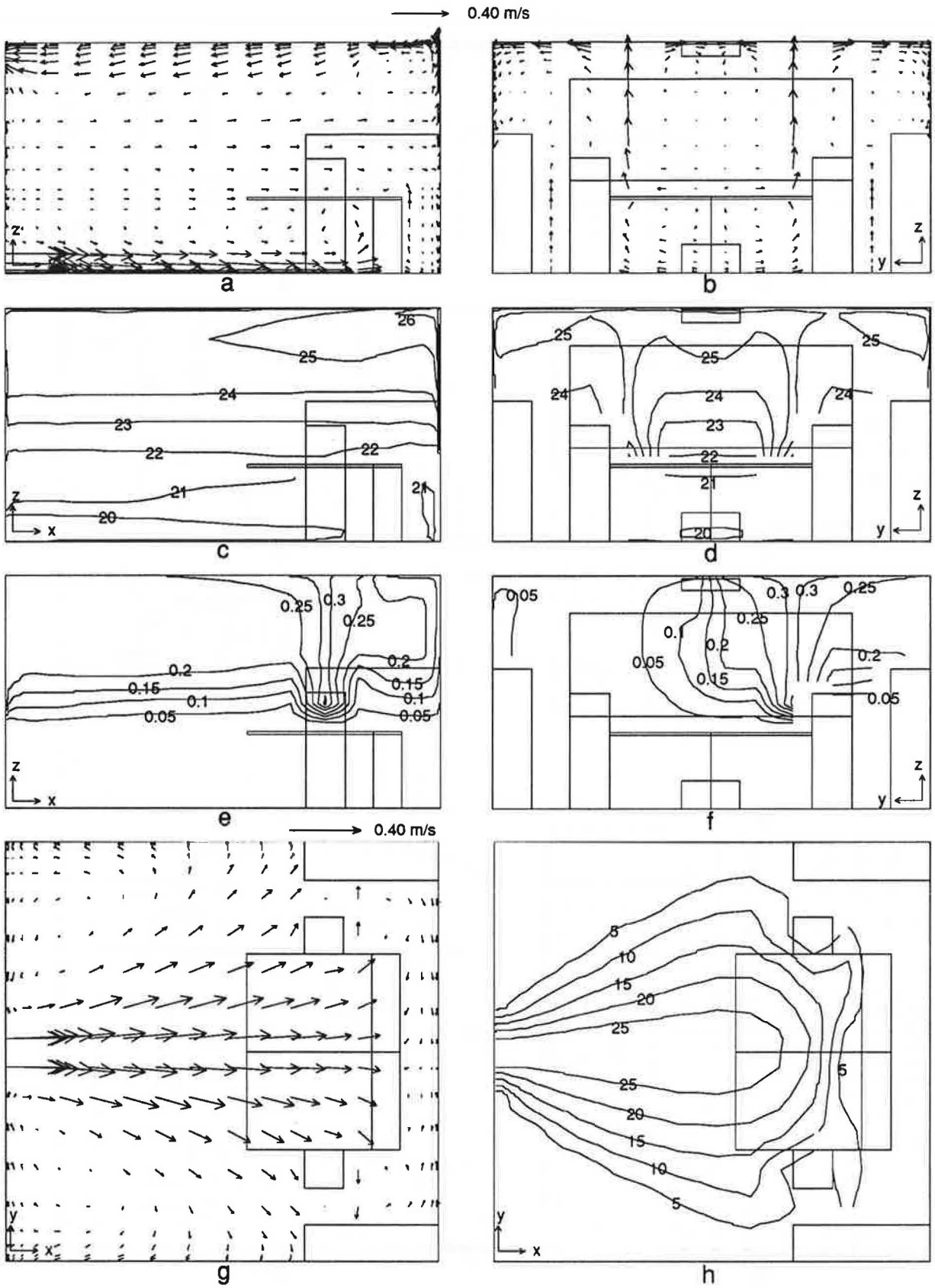

Figure 5. Computed field distributions with a smaller inlet height. (a) velocity in section I-I; (b) velocity in section III-III; (c) temperature in section I-I [℃]; (d) temperature in section III-III [℃]; (e) smoke concentration in section II-II [ppm]; (f) smoke concentration in section III-III [ppm]; (g) velocity in 0.05 m above the floor (top view); (h) percentage dissatisfied people due to draft in 0.05 m above the floor (top view) [%].

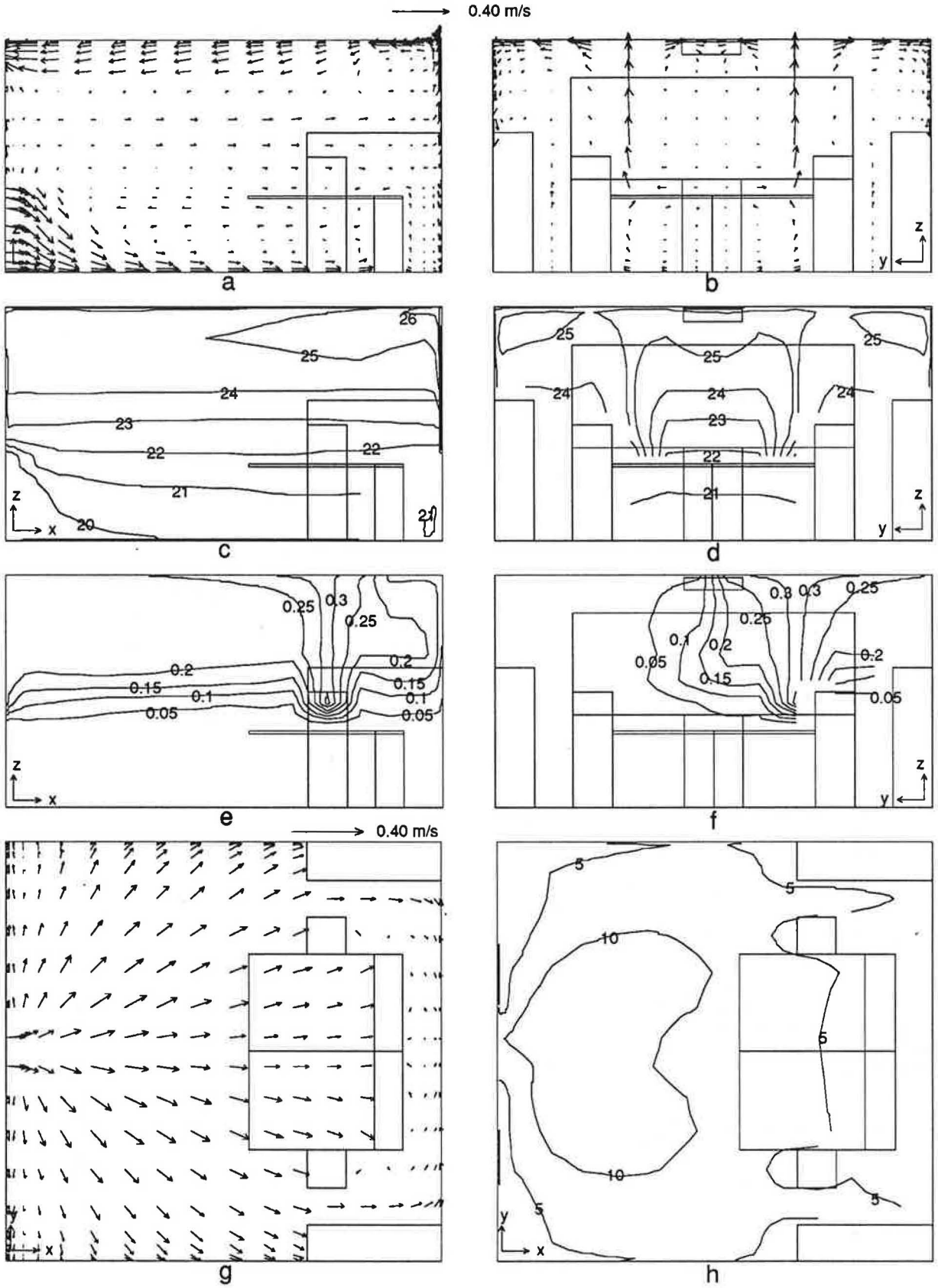

Figure 6. Computed field distributions with a larger inlet height. (a) velocity in section I-I; (b) velocity in section III-III; (c) temperature in section I-I [℃]; (d) temperature in section III-III [℃]; (e) smoke concentration in section II-II [ppm]; (f) smoke concentration in section III-III [ppm]; (g) velocity in 0.05 m above the floor (top view); (h) percentage dissatisfied people due to draft in 0.05 m above the floor (top view) [%].

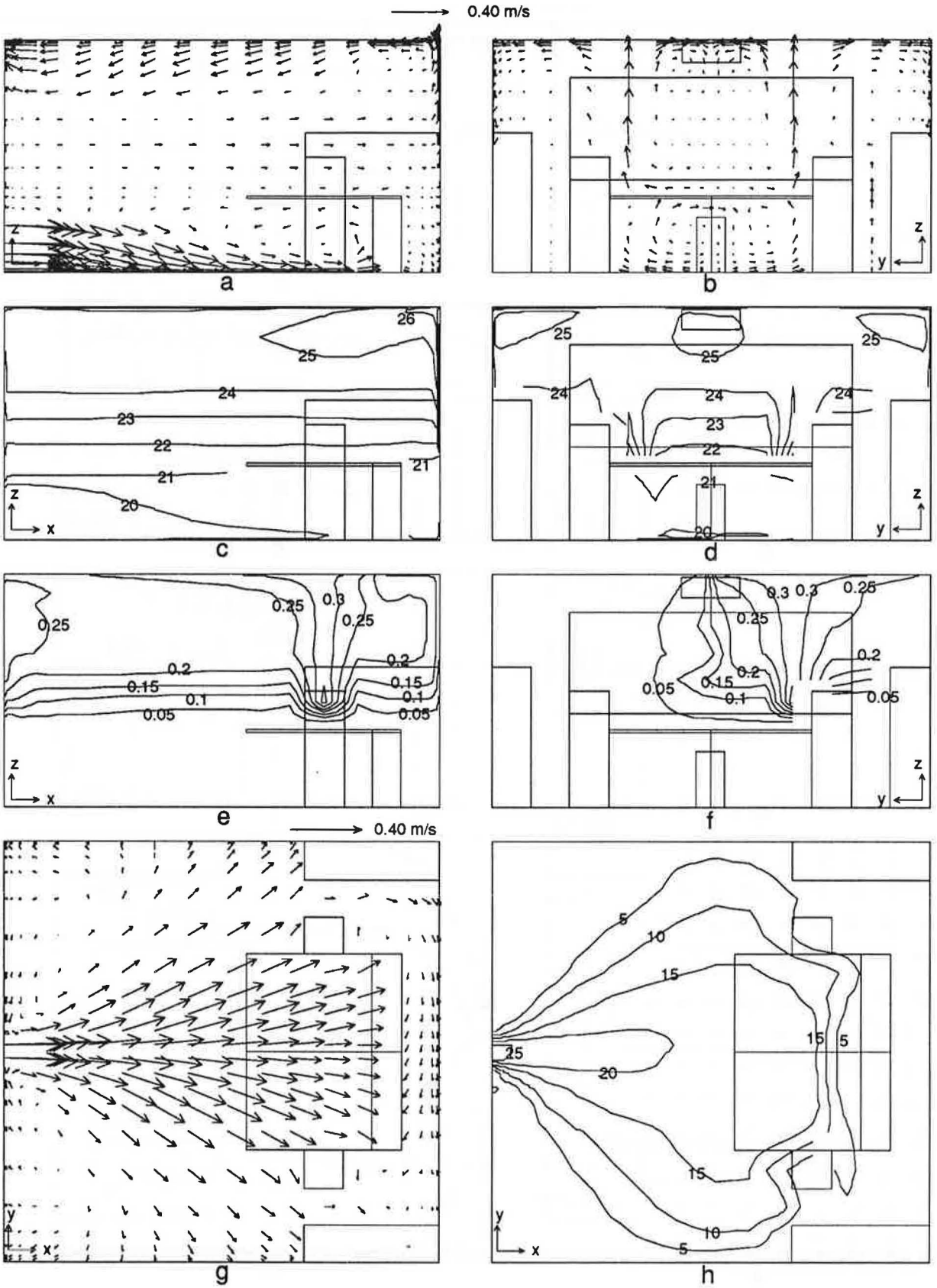

Figure 7. Computed field distributions with a smaller inlet width. (a) velocity in section I-I; (b) velocity in section III-III; (c) temperature in section I-I [℃]; (d) temperature in section III-III [℃]; (e) smoke concentration in section II-II [ppm]; (f) smoke concentration in section III-III [ppm]; (g) velocity in 0.05 m above the floor (top view); (h) percentage dissatisfied people due to draft in 0.05 m above the floor (top view) [%].

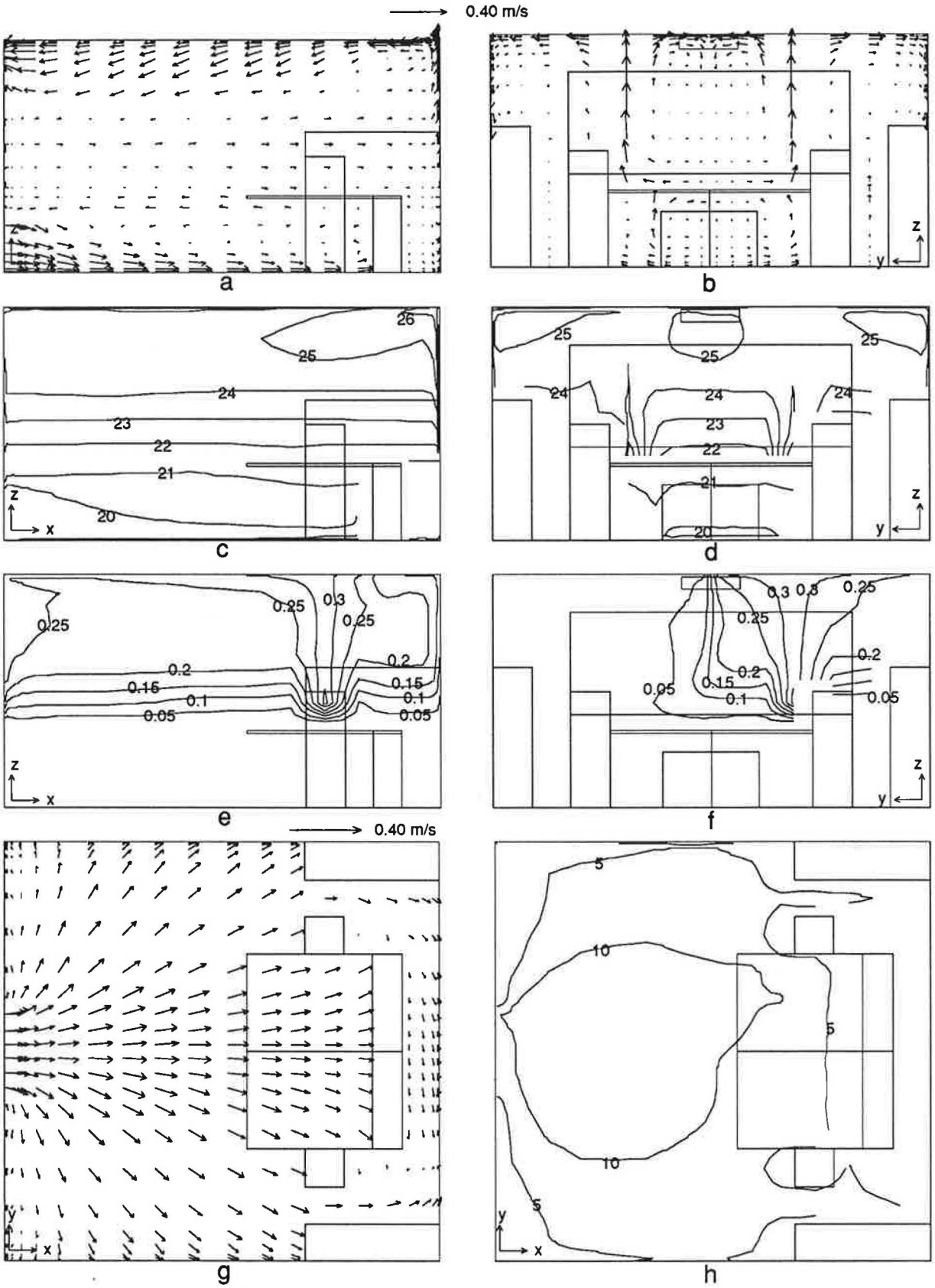

Figure 8. Computed field distributions with a larger inlet width. (a) velocity in section I-I; (b) velocity in section III-III; (c) temperature in section I-I [℃]; (d) temperature in section III-III [℃]; (e) smoke concentration in section II-II [ppm]; (f) smoke concentration in section III-III [ppm]; (g) velocity in 0.05 m above the floor (top view); (h) percentage dissatisfied people due to draft in 0.05 m above the floor (top view) [%].

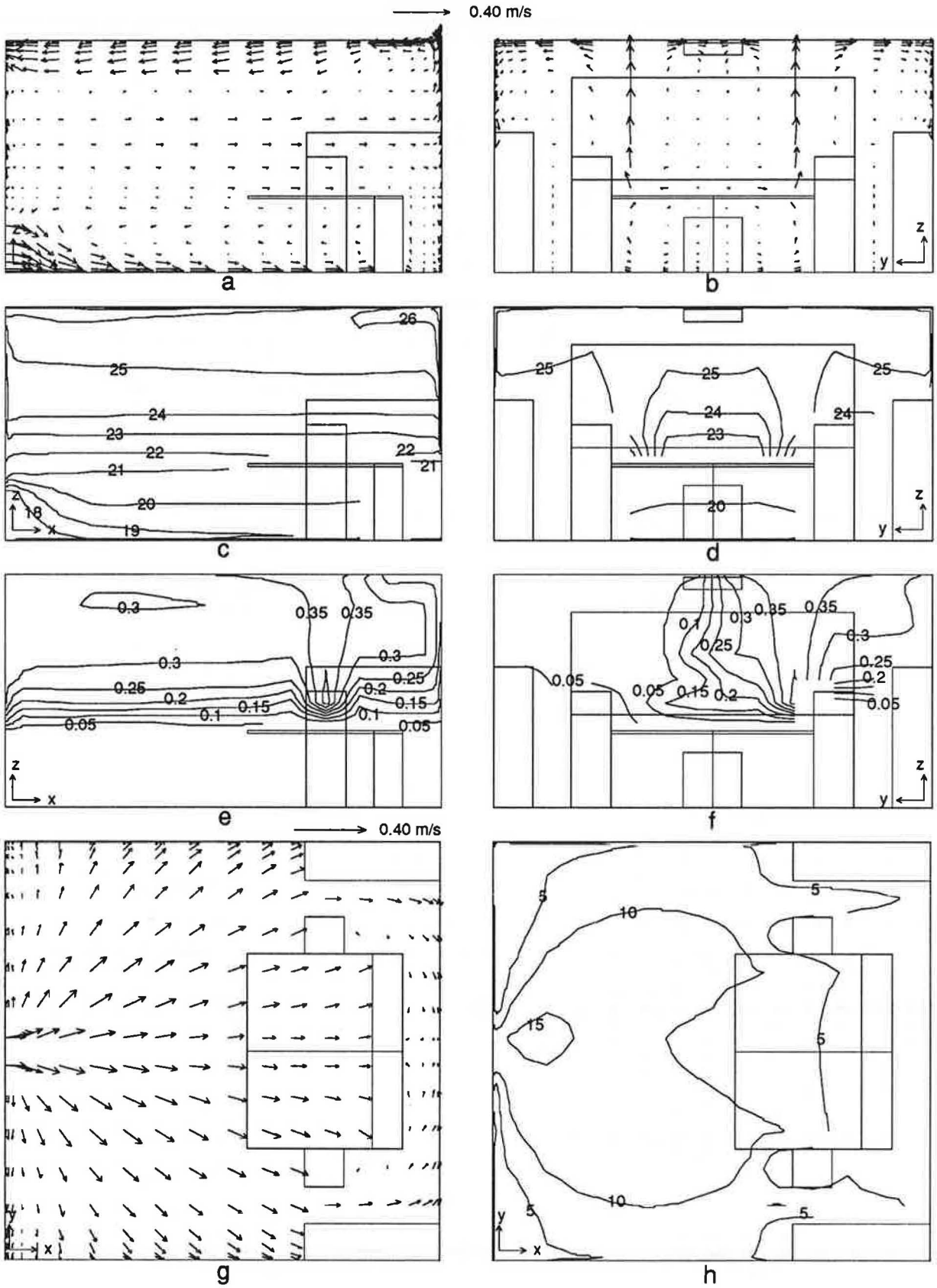

Figure 9. Computed field distributions with a smaller ventilation rate and a lower supply temperature. (a) velocity in section I-I; (b) velocity in section III-III; (c) temperature in section I-I [℃]; (d) temperature in section III-III [℃]; (e) smoke concentration in section II-II [ppm]; (f) smoke concentration in section III-III [ppm]; (g) velocity in 0.05 m above the floor (top view); (h) percentage dissatisfied people due to draft in 0.05 m above the floor (top view) [%].

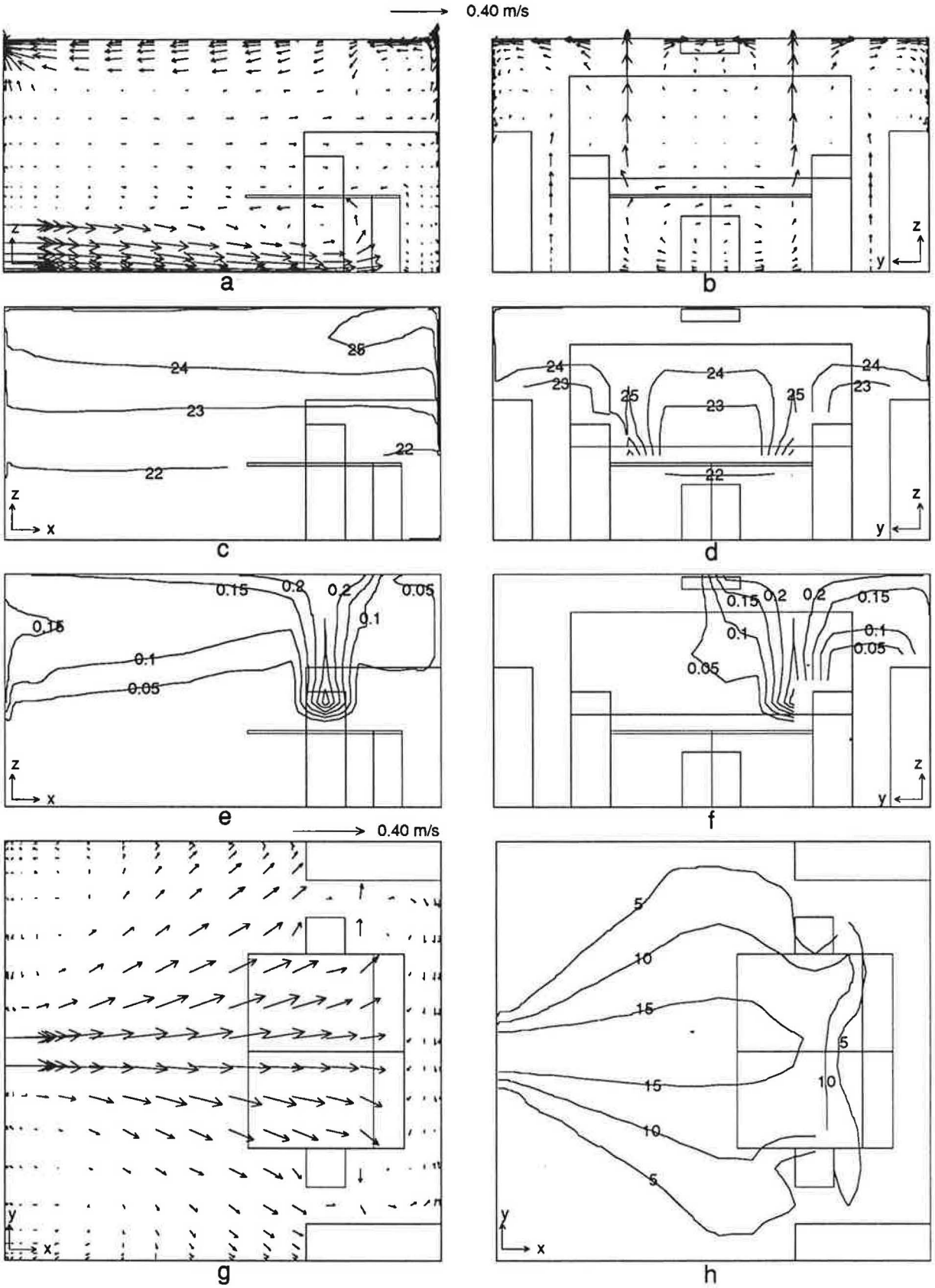

Figure 10. Computed field distributions with a larger ventilation rate and a higher supply temperature. (a) velocity in section I-I; (b) velocity in section III-III; (c) temperature in section I-I [℃]; (d) temperature in section III-III [℃]; (e) smoke concentration in section II-II [ppm]; (f) smoke concentration in section III-III [ppm]; (g) velocity in 0.05 m above the floor (top view); (h) percentage dissatisfied people due to draft in 0.05 m above the floor (top view) [%].